Electronic Supplementary Information (ESI)

Levulinic Acid-Based Bioplasticizers: a Facile Approach to Enhance Thermal and Mechanical Properties of Polyhydroxyalkanoates

Alessandro Sinisi [a], Micaela Degli Esposti [a,b,], Simona Braccini [c], Federica Chiellini [c], Susana Guzman-Puyol [d], José Alejandro Heredia-Guerrero [d], Davide Morselli [a,b,*] and Paola Fabbri [a,b]*

[a] Department of Civil Chemical, Environmental and Materials Engineering (DICAM), Università di Bologna, Via Terracini 28, Bologna 40131, Italy

[b] National Interuniversity Consortium of Materials Science and Technology (INSTM), Via Giusti 9, Firenze 50121, Italy

[c] Department of Chemistry and Industrial Chemistry, Università di Pisa, Via G. Moruzzi 13, 56124 Pisa, Italy

[d] Instituto de Hortofruticultura Subtropical y Mediterránea "La Mayora", Universidad de Málaga-Consejo Superior de Investigaciones Científicas (IHSM, UMA-CSIC), Av. Louis Pasteur, 49, 29010 Málaga, Spain

Corresponding authors: davide.morselli6@unibo.it; micaela.degliesposti@unibo.it

FT-IR experimental details

The chemical structures of the intermediates and the final ketal-diesters were characterized by FT-IR spectroscopy. Spectra were recorded on a PerkinElmer Spectrum Two spectrometer equipped with a diamond crystal in Attenuated Total Reflectance (ATR) mode. Measurements were carried out in the range of 4000 to 400 cm^{-1} at room temperature; the spectral resolution was 4 cm^{-1} and the number of scans was 64 for each spectrum. Spectra were processed with Spectrum 10 software (PerkinElmer).

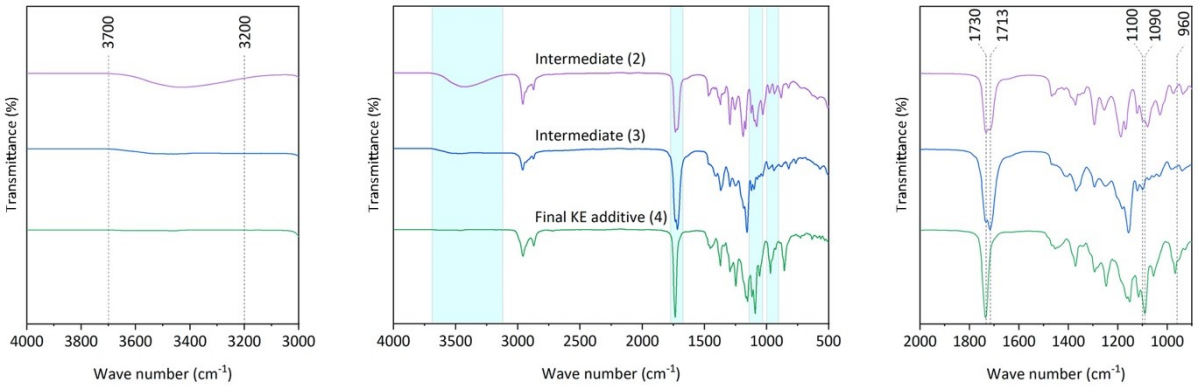

Figure S1. Representative FT-IR spectra of the intermediates and relative final ketal-ester KE-myr. On the left, it is reported the range between 4000 and 3000 cm^{-1} and on the right the range between 2000 and 900 cm^{-1}. The dashed lines indicate the most characteristic absorption peaks that change during the synthesis.

FT-IR assignments

Broad peak between 3700 to 3200 cm^{-1} associated with O−H stretching vibration disappears due to the formation of the ester with levulinic acid. Moreover, beyond the characteristic peak at 1730 cm^{-1} (ester C=O stretching), a peak at 1713 cm^{-1} is observed, revealing the simultaneous presence of a keto group introduced to levulinic acid. This signal is not more detectable in the final molecule. On the other hand, new peaks appear at 1100, 1090, and 960 cm^{-1} (alkoxy C−O stretching), confirming the occurrence of the reaction between the keto group and 1,3-propanediol that results in the ketal formation.[1]

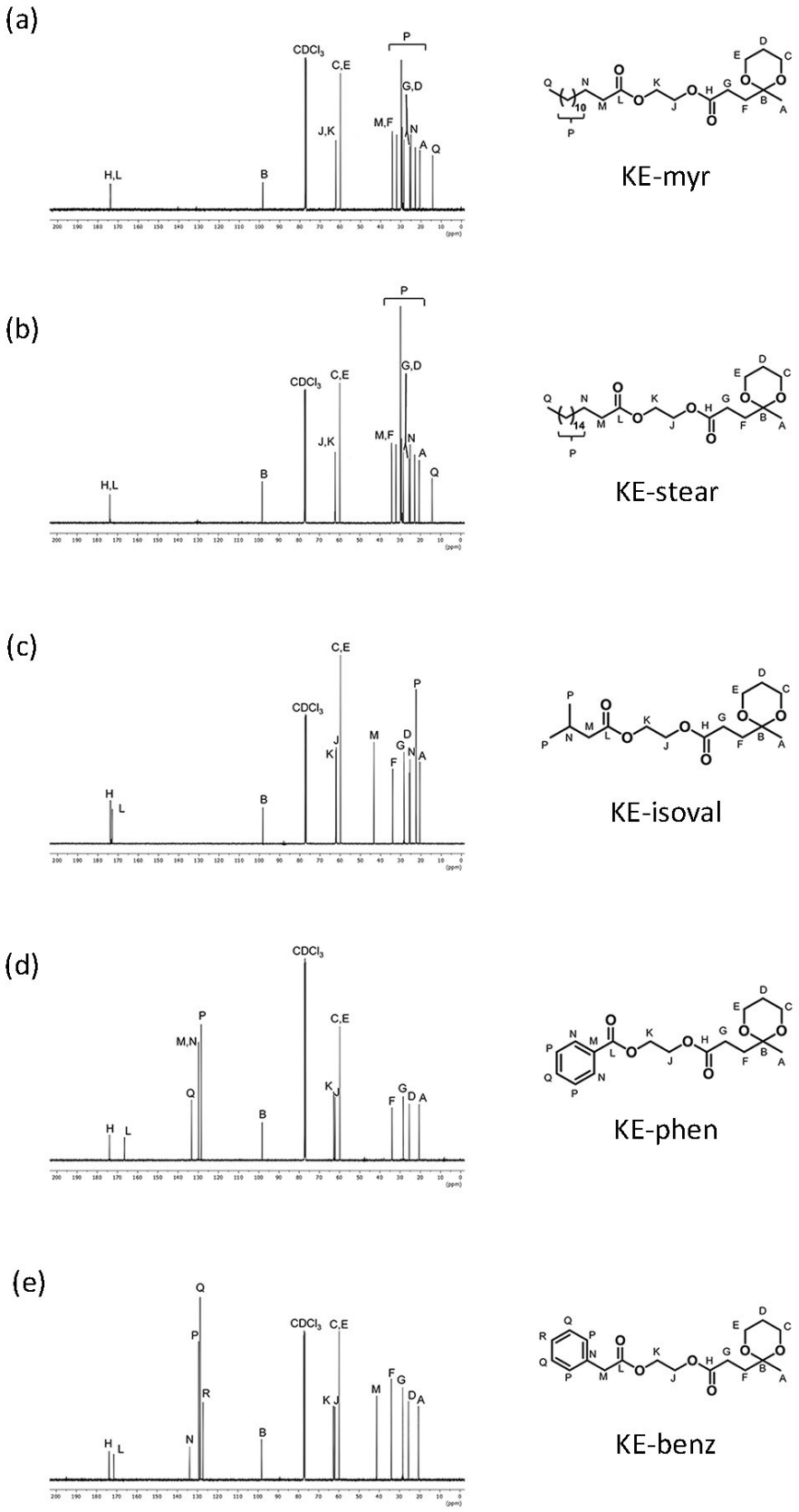

Figure S2. ^{13}C-NMR spectra with corresponding carbon assignments of final ketal-esters (a) KE-myr, (b) KE-stear, (c) KE-isoval, (d) KE-phen and (e) KE-benz.[1]

Yields, ^{1}H- and ^{13}C-NMR assignments of the final bioplasticizers

KE-myr:

[$CH_3(CH_2)_{10}CH_2CH_2C(=O)OCH_2CH_2O(O=)CCH_2CH_2C(-OCH_2CHH'CH_2O-)CH_3$], 58% yield, colorless oil.

^{1}*H-NMR* ($CDCl_3$, 400 MHz) δ = 4.27 (s, 4H, OCH_2CH_2O), 3.96-3.80 (m, 4H, $C(-OCH_2CHH'CH_2O-)$), 2.49 (t, 2H, $O(O=)CCH_2CH_2$), 2.32 (t, 2H, $CH_2CH_2C(=O)O$), 2.03 (t, 2H, $O(O=)CCH_2CH_2$), 1.87-1.75 (m, 1H, $C(-OCH_2CHH'CH_2O-)$), 1.67-1.58 (m, 2H, $CH_2CH_2C(=O)O$), 1.56-1.49 (m, 1H, $C(-OCH_2CHH'CH_2O-)$), 1.41 (s, 3H, $C(-OCH_2CHH'CH_2O-)CH_3$), 1.34-1.21 (m, 20H, $CH_3(CH_2)_{10}$), 0.88 (t, 3H, $CH_3(CH_2)_{10}$) ppm.

^{13}*C-NMR* ($CDCl_3$, 150 MHz δ = 173.83 ($O(O=)CCH_2CH_2$), 173.77 ($CH_2CH_2C(=O)O$), 98.1 ($C(-OCH_2CHH'CH_2O-)$), 62.3 (OCH_2CH_2O), 62.1 (OCH_2CH_2O), 59.9 ($C(-OCH_2CHH'CH_2O-)$), 34.3 ($CH_2CH_2C(=O)O$), 34.1 ($O(O=)CCH_2CH_2$), 32.0 ($CH_3(CH_2)_{10}$), 29.7 ($CH_3(CH_2)_{10}$), 29.78 ($CH_3(CH_2)_{10}$), 29.75 ($CH_3(CH_2)_{10}$), 29.6 ($CH_3(CH_2)_{10}$), 29.5 ($CH_3(CH_2)_{10}$), 29.4 ($CH_3(CH_2)_{10}$), 29.3 ($CH_3(CH_2)_{10}$), 28.5 ($O(O=)CCH_2CH_2$), 25.5 ($C(-OCH_2CHH'CH_2O-)$), 25.0 ($CH_2CH_2C(=O)O$), 22.8 ($CH_3(CH_2)_{10}$), 20.6 ($C(-OCH_2CHH'CH_2O-)CH_3$), 14.1 ($CH_3(CH_2)_{10}$) ppm.

KE-stear:

[$CH_3(CH_2)_{14}CH_2CH_2C(=O)OCH_2CH_2O(O=)CCH_2CH_2C(-OCH_2CHH'CH_2O-)CH_3$], 63% yield, colorless oil.

^{1}*H-NMR* ($CDCl_3$, 400 MHz) δ = 4.27 (s, 4H, OCH_2CH_2O), 3.97-3.80 (m, 4H, $C(-OCH_2CHH'CH_2O-)$), 2.47 (t, 2H, $O(O=)CCH_2CH_2$), 2.32 (t, 2H, $CH_2CH_2C(=O)O$), 2.03 (t, 2H, $O(O=)CCH_2CH_2$), 1.86-1.74 (m, 1H, $C(-OCH_2CHH'CH_2O-)$), 1.68-1.60 (m, 2H, $CH_2CH_2C(=O)O$), 1.56-1.49 (m, 1H, $C(-OCH_2CHH'CH_2O-)$), 1.40 (s, 3H, $C(-OCH_2CHH'CH_2O-)CH_3$), 1.34-1.22 (m, 28H, $CH_3(CH_2)_{14}$), 0.88 (t, 3H, $CH_3(CH_2)_{14}$) ppm.

^{13}*C-NMR* ($CDCl_3$, 150 MHz) δ = 173.82 ($O(O=)CCH_2CH_2$), 173.76 ($CH_2CH_2C(=O)O$), 98.3 ($C(-OCH_2CHH'CH_2O-)$), 62.1 (OCH_2CH_2O), 62.1 (OCH_2CH_2O), 59.9 ($C(-OCH_2CHH'CH_2O-)$), 34.3 ($CH_2CH_2C(=O)O$), 34.1 ($O(O=)CCH_2CH_2$), 32.1 ($CH_3(CH_2)_{14}$), 29.83 ($CH_3(CH_2)_{14}$), 29.82 ($CH_3(CH_2)_{14}$), 29.79 ($CH_3(CH_2)_{14}$), 29.75 ($CH_3(CH_2)_{14}$), 29.6 ($CH_3(CH_2)_{14}$), 29.6 ($CH_3(CH_2)_{14}$), 29.4 ($CH_3(CH_2)_{14}$), 29.3 ($CH_3(CH_2)_{14}$), 28.5 ($O(O=)CCH_2CH_2$), 25.5 ($C(-OCH_2CHH'CH_2O-)$), 25.0 ($CH_2CH_2C(=O)O$), 22.8 ($CH_3(CH_2)_{14}$), 20.6 ($C(-OCH_2CHH'CH_2O-)CH_3$), 14.2 ($CH_3(CH_2)_{14}$) ppm.

KE-isoval:

[$(CH_3)_2CHCH_2C(=O)OCH_2CH_2O(O=)CCH_2CH_2C(-OCH_2CHH'CH_2O-)CH_3$], 55% yield, colorless oil.

^{1}H-NMR ($CDCl_3$, 400 MHz) δ = 4.27 (s, 4H, OCH_2CH_2O), 3.97-3.81 (m, 4H, $C(-OCH_2CHH'CH_2O-)$), 2.48 (t, 2H, $O(O=)CCH_2CH_2$), 2.21 (d, 2H, $(CH_3)_2CHCH_2$), 2.16-2.06 (m, 1H, $(CH_3)_2CHCH_2$), 2.03 (t, 2H, $O(O=)CCH_2CH_2$), 1.85-1.73 (m, 1H, $C(-OCH_2CHH'CH_2O-)$), 1.58-1.49 (m, 1H, $C(-OCH_2CHH'CH_2O-)$), 1.40 (s, 3H, $C(-OCH_2CHH'CH_2O-)CH_3$), 0.97 (d, 6H, $(CH_3)_2CH$) ppm.

^{13}C-NMR ($CDCl_3$, 150 MHz) δ = 173.8 ($O(O=)CCH_2CH_2$), 173.0 ($(CH_3)_2CHCH_2C(=O)O$), 98.1 ($C(-OCH_2CHH'CH_2O-)$), 62.2 (OCH_2CH_2O), 62.0 (OCH_2CH_2O), 59.9 ($C(-OCH_2CHH'CH_2O-)$), 43.3 ($(CH_3)_2CHCH_2C(=O)O$), 34.0 ($O(O=)CCH_2CH_2$), 28.3 ($O(O=)CCH_2CH_2$), 25.8 ($C(-OCH_2CHH'CH_2O-)$), 25.5 ($(CH_3)_2CHCH_2C(=O)O$), 22.5 ($(CH_3)_2CHCH_2C(=O)O$), 20.6 ($C(-OCH_2CHH'CH_2O-)CH_3$) ppm.

KE-phen:

[$C_6H_5C(=O)OCH_2CH_2O(O=)CCH_2CH_2C(-OCH_2CHH'CH_2O-)CH_3$], 52% yield, colorless oil.

^{1}H-NMR ($CDCl_3$, 400 MHz) δ = 8.05 (d, 2H, *ortho*), 7.57 (t, 1H, *para*), 7.45 (t, J = 7.9 Hz, 2H, *meta*), 4.56-4.49 (m, 2H, OCH_2CH_2O), 4.45-4.39 (m, 2H, OCH_2CH_2O), 3.95-3.77 (m, 4H, $C(-OCH_2CHH'CH_2O-)$), 2.50 (t, 2H, $O(O=)CCH_2CH_2$), 2.04 (t, 2H, $O(O=)CCH_2CH_2$), 1.83-1.70 (m, 1H, $C(-OCH_2CHH'CH_2O-)$), 1.55-1.45 (m, 1H, $C(-OCH_2CHH'CH_2O-)$), 1.39 (s, 3H, $C(-OCH_2CHH'CH_2O-)CH_3$) ppm.

^{13}C-NMR ($CDCl_3$, 150 MHz) δ =173.9 ($O(O=)CCH_2CH_2$), 166.5 ($C_6H_5C(=O)O$), 133.3 (*para* carbon), 130.0 (quaternary aromatic carbon), 129.8 (*ortho* carbons), 128.5 (*meta* carbon), 98.3 ($C(-OCH_2CHH'CH_2O-)$), 62.9 (OCH_2CH_2O), 62.2 (OCH_2CH_2O), 59.9 ($C(-OCH_2CHH'CH_2O-)$), 34.1 ($O(O=)CCH_2CH_2$), 28.5 ($O(O=)CCH_2CH_2$), 25.4 ($C(-OCH_2CHH'CH_2O-)$), 20.6 ($C(-OCH_2CHH'CH_2O-)CH_3$) ppm.

KE-benz:

[$C_6H_5CH_2C(=O)OCH_2CH_2O(O=)CCH_2CH_2C(-OCH_2CHH'CH_2O-)CH_3$], 54% yield, colorless oil.

^{1}H-NMR ($CDCl_3$, 400 MHz) δ = 7.35-7.27 (m, 5H, C_6H_5), 4.32-4.25 (m, 4H, OCH_2CH_2O), 3.97-3.81 (m, 4H, $C(-OCH_2CHH'CH_2O-)$), 3.65 (s, 2H, $C_6H_5CH_2C(=O)O$), 2.46 (t, 2H, $O(O=)CCH_2CH_2$), 2.02 (t, 2H, $O(O=)CCH_2CH_2$), 1.86-1.74 (m, 1H, $C(-OCH_2CHH'CH_2O-)$), 1.58-1.49 (m, 1H, $C(-OCH_2CHH'CH_2O-)$), 1.40 (s, 3H, $C(-OCH_2CHH'CH_2O-)CH_3$) ppm.

^{13}C-NMR ($CDCl_3$, 150 MHz) δ = 173.8 ($O(O=)CCH_2CH_2$), 171.5 ($C_6H_5CH_2C(=O)O$), 133.9 (quaternary aromatic carbon), 129.4 (*para* carbon), 128.7 (*ortho* carbons), 127.3 (*meta*

carbons), 98.3 (*C*(-$OCH_2CHH'CH_2O$-)), 62.6 (OCH_2CH_2O), 62.0 (OCH_2CH_2O), 59.9 (C(-$OCH_2CHH'CH_2O$-)), 41.3 ($C_6H_5CH_2C(=O)O$), 34.0 ($O(O=)CCH_2CH_2$), 28.4 ($O(O=)CCH_2CH_2$), 25.4 (C(-$OCH_2CHH'CH_2O$-)), 20.6 (C(-$OCH_2CHH'CH_2O$-)CH_3) ppm.

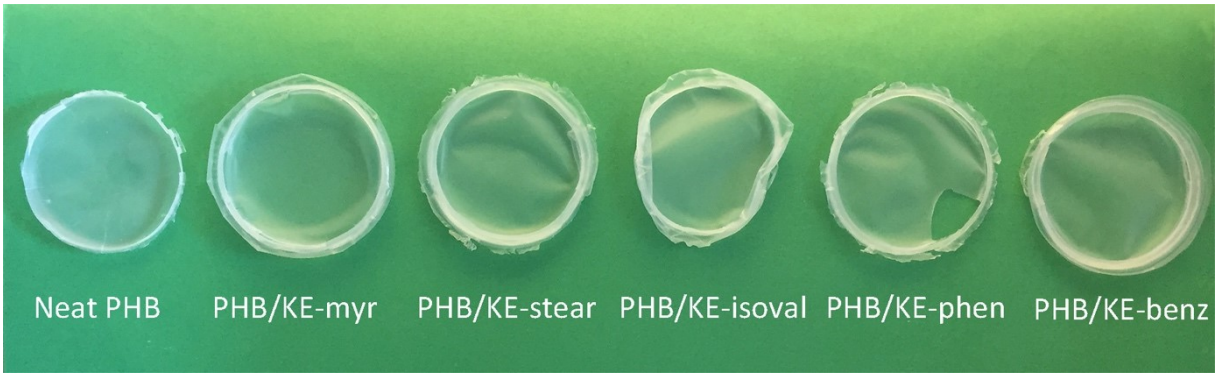

Figure S3. Photographs of neat and compounded PHB films obtained by solvent-casting.

Table S1. Glass transition temperature (T_g), melting temperature (T_m) and storage modulus *(E')* at 25°C of neat and plasticized PHB films.

	T_g [°C]		**T_m [°C]**		***E'* [MPa]**	
PHB	0.2±0.2		170.5±0.5		3032±26	
Sample	**10 phr**	**20 phr**	**10 phr**	**20 phr**	**10 phr**	**20 phr**
PHB/KE-myr	-12.0±0.2	-16.3±0.2	167.7±0.7	165.7±0.2	2625±101	2011±51
PHB/KE-stear	-4.0±0.2	-6.2±0.2	167.7±0.2	165.8±0.2	2097±158	1832±185
PHB/KE-isoval	-4.9±0.2	-9.3±0.2	169.7±0.3	164.1±0.1	2491±15	1783±108
PHB/KE-phen	-7.7±0.2	-16.8±0.2	168.7±0.3	162.3±0.2	2417±182	1600±32
PHB/KE-benz	-9.6±0.2	-16.5±0.2	169.2±0.2	161.3±0.4	2538±126	1583±21

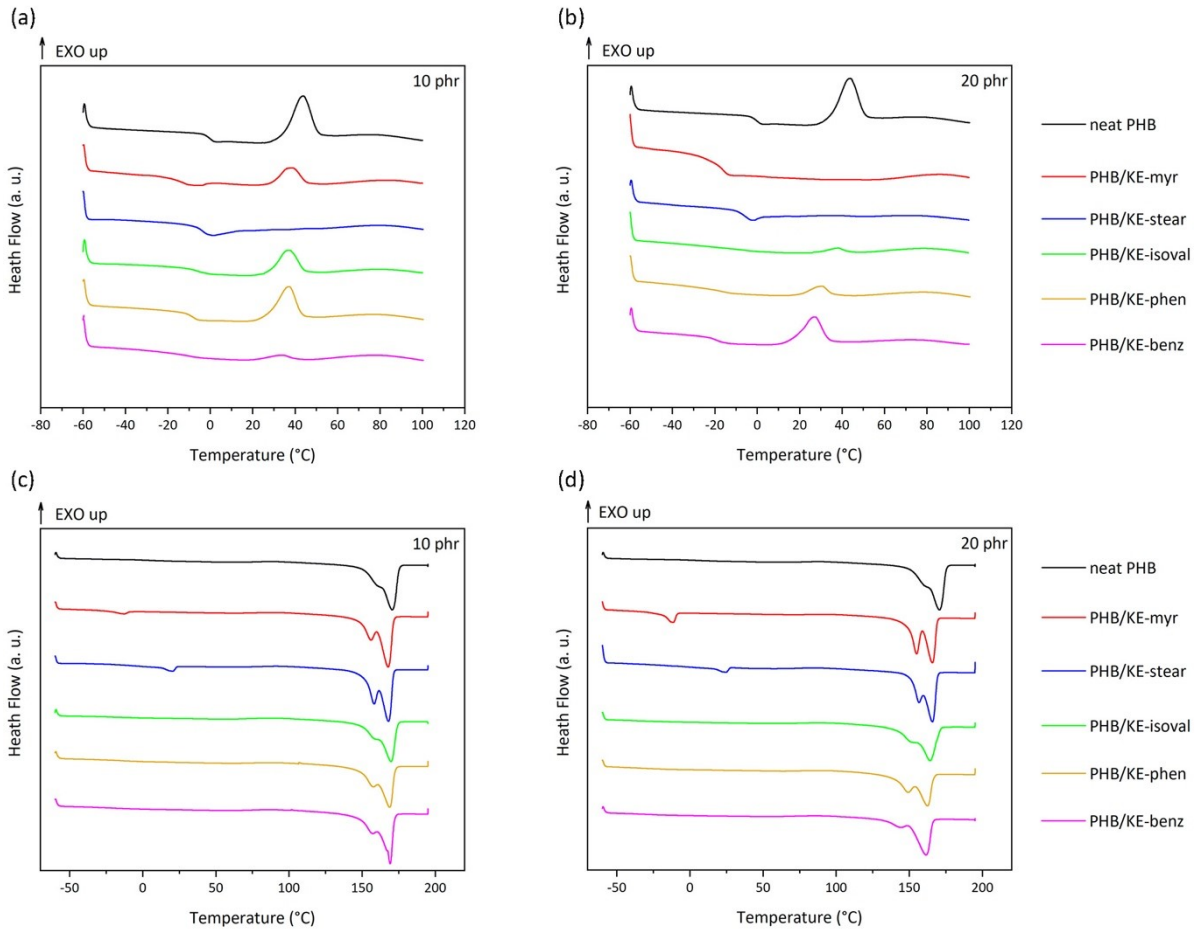

Figure S4. DSC curves recorded from the third heating scan of neat and compounded PHB films with (a) 10 phr and (b) 20 phr of additive content. DSC curves recorded from the second heating scan of neat and compounded PHB films with (c) 10 phr and (d) 20 phr of additive.

Table S2. Enthalpy of melting (ΔH_m) and degree of crystallinity (χ) calculated by Equation 2.

	ΔH_m [J·g^{-1}]		**χ [%]**	
PHB	89.81 ± 0.33		61.5 ± 0.5	
Sample	**10 phr**	**20 phr**	**10 phr**	**20 phr**
PHB/KE-myr	90.50 ± 0.53	87.05 ± 1.25	68.0 ± 1.7	71.6 ± 1.5
PHB/KE-stear	78.25 ± 0.05	72.67 ± 0.69	59.0 ± 1.1	60.0 ± 1.1
PHB/KE-isoval	81.09 ± 0.44	78.57 ± 0.37	61.1 ± 1.4	64.9 ± 0.6
PHB/KE-phen	83.86 ± 0.53	73.55 ± 0.48	63.2 ± 1.8	60.1 ± 0.2
PHB/KE-benz	87.29 ± 0.60	70.84 ± 0.79	66.06 ± 1.9	58.2 ± 0.7

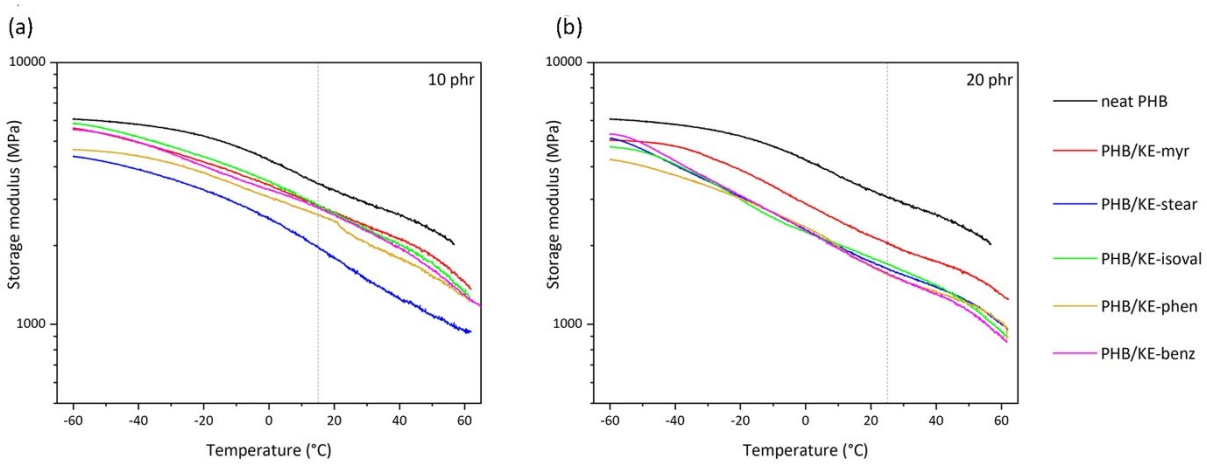

Figure S5. Storage modulus *(E' at log scale)* as a function of the temperature of neat and compounded PHB films with (a) 10 phr and (b) 20 phr of additive. The dashed lines indicate 25°C that is the temperature at which *E'* values were extrapolated.

Table S3. Summary of the data obtained by cytocompatibility tests on neat and plasticized PHB with 20 phr of additive.

	Cell viability [%]	
Sample	**Extract diluted 1:2**	**Extract diluted 1:4**
PHB	106.4 ± 10.1	107.2 ± 5.2
PHB/KE-myr	104.7 ± 13.8	109.1 ± 6.6
PHB/KE-stear	90.9 ± 4.9	99.5 ± 6.2
PHB/KE-isoval	40.3 ± 11.0	99.3 ± 10.7
PHB/KE-phen	67.5 ± 6.8	90.2 ± 7.8
PHB/KE-benz	85.0 ± 9.7	92.1 ± 11.8

GPC experimental details

Molecular weights of the purified PHB (as described elsewhere[2]) were determined by gel permeation chromatography (GPC) with an Agilent 1260 Infinity instrument (G1322A 1260 Degasser, G1310B 1260 Isocratic Pump, G1316A 1260 TCC Thermostatted Column Compartment, G1362A 1260 RID Reflective Index Detector, G1328C 126 Manual Injector); RID and column compartment were thermostatically controlled at 35°C ± 0.2°C. The instrument

was equipped with a PLgel MiniMIX-A column (20 µm particle size, 4.6×250mm) coupled with a Tosoh TSKgel SuperMultipore HZ-M column (4 µm particle size, 4.6 ×150mm); columns were preceded by a low dispersion in-line filter (frit porosity 0.2 µm). $CHCl_3$ was used as mobile phase at a flow rate of 0.2 mL·min^{-1} and toluene was used as internal standard (0.1 µL·mL^{-1}), run time of 37 minutes. Results were processed with Agilent GPC/SEC software, version A.02.01 using a calibration curve obtained with monodispersed polystyrene standards (EasiCal PS-1 Agilent kit).

NMR experimental details

Structure of purified PHB (as described elsewhere[2]) was determined by proton nuclear magnetic resonance (^{1}H-NMR) using an FT-NMR Avance400 400 MHz spectrometer (Bruker). Spectrum was recorded at room temperature using approximately 10 mg of purified polymer dissolved in 0.85 mL of deuterated chloroform. Data was processed with Bruker TopSpin software, version 4.0.7.

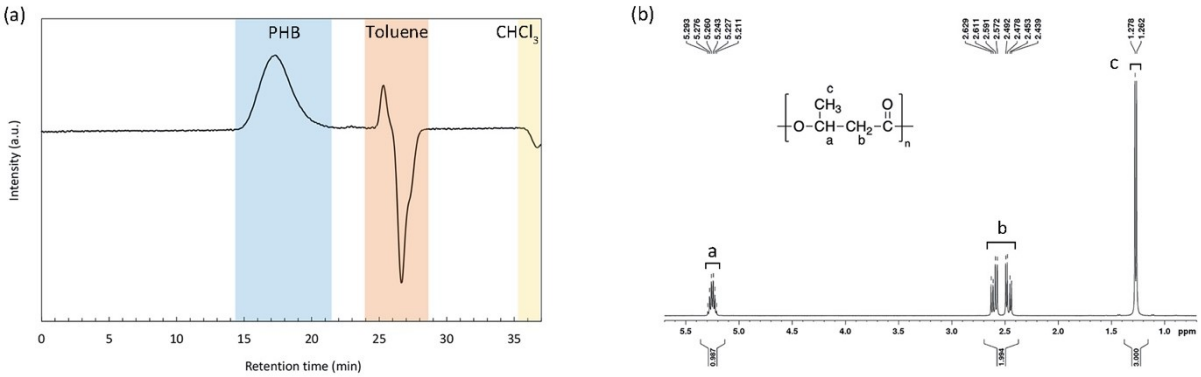

Figure S6. (a) GPC chromatogram of the purified PHB. Blue, orange and yellow rectangles indicate the signals associated to polymer, reference (toluene) and solvent ($CHCl_3$), respectively. (b) ^{1}H-NMR spectrum and related signals assignment (chemical shifts are reported in ppm relative to residual $CHCl_3$ signal at 7.26 ppm) and integrals collected analyzing the purified PHB used for the film preparation.

Table S4. Peak molecular weight (M_p), number average molecular weight (M_n), weight average molecular weight (M_w) and polydispersity (P, calculated as M_w/M_n) as determined by gel permeation chromatography.

M_p [g·mol^{-1}]	M_n [g·mol^{-1}]	M_w [g·mol^{-1}]	P
170000	71600	245100	3.42

References

1 A. Sinisi, M. Degli Esposti, M. Toselli, D. Morselli and P. Fabbri, *ACS Sustain. Chem. Eng.*, **2019**, 7, 13920–13931.

2 M. Degli Esposti, F. Chiellini, F. Bondioli, D. Morselli and P. Fabbri, *Mater. Sci. Eng. C*, **2019**, 100, 286–296.